MODELING OF FUEL BUNDLE VIBRATION AND THE ASSOCIATED FRETTING WEAR IN A CANDU FUEL CHANNEL

A. Mohany

Fluid-Sound-Structure Interaction Laboratory University of New Brunswick, New Brunswick, Canada amohany@unb.ca

and

M. Hassan

Flow-Induced Vibration Laboratory University of Guelph, Ontario, Canada mahassan@uoguelph.ca

Abstract

In this paper a numerical model is developed to predict the vibration response of a CANDU® fuel bundle and the associated fretting wear in the surrounding pressure tube. One excitation mechanism is considered in this model; turbulence-induced excitation caused by coolant flow inside the fuel channel. The numerical model can be easily adapted to include the effects of seismic events, fuel bundle impact during refuelling and start-up of the reactor, and the acoustic pressure pulsations caused by the primary heat transport (PHT) pumps. The simulation is performed for a typical CANDU fuel bundle with 37 fuel elements. The clearances between the buttons of the inner fuel elements, and between the bearing pads of the outer fuel elements and the pressure tube were measured from an actual fuel bundle. Some variability among the measured clearance values was observed. Therefore, probability density functions of the measured clearance values were established and the simulation was performed for the probabilistic distribution of the clearance values. The contact between the fuel bundle and the pressure tube is modeled using pseudo-force contact method. The proposed modelling technique can be used in future CANDU reactors to avoid fuel and pressure tube fretting damage due to the aforementioned excitation mechanisms

Introduction

Fuel bundles are one of the most important design elements of any nuclear reactor. Therefore, it is crucial to ensure safe and reliable operation of nuclear fuel bundles during their expected lifetime in the reactor. In CANDU (CANadia Deuterium Uranium) reactors the fuel bundle consists of 37 parallel fuel elements, as shown in Figure 1. Two endplates, shown in Figure 2, are designed to keep the fuel elements intact. The length of each fuel bundle is approximately 0.5 m and its diameter is about 0.1 m. Bearing pads are attached to the outer fuel elements at

[•] CANDU is a registered trade-mark of Atomic Energy of Canada Limited (AECL).

three different locations along the length of the bundle to prevent contact between the fuel bundle and the surrounding pressure tube, as shown in Figure 1. Moreover, different types of contact buttons are attached to the inner fuel elements to maintain the spacing between them and to minimize any excessive vibrations that could lead to fuel elements damage. A CANDU 6 reactor has 380 horizontal fuel channels and each fuel channel has 12 fuel bundles. Heavy water coolant flows inside the fuel channels to remove heat generated by the fission reaction. Therefore, Flow-induced vibration is considered to be an important factor in the design process of CANDU fuel bundles.

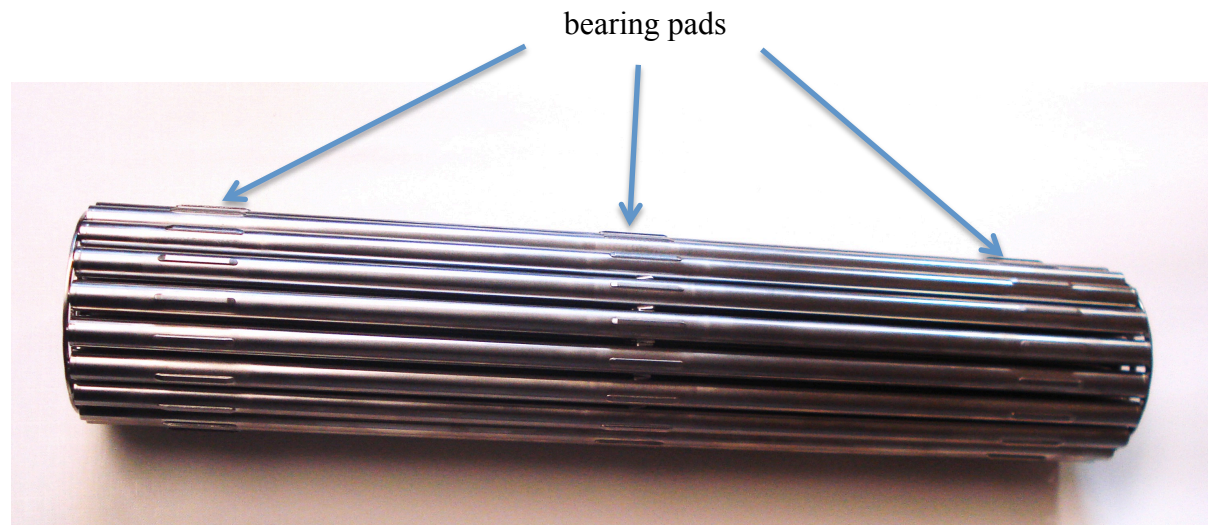


Figure 1: Typical CANDU fuel bundle with the bearing pads attached to the outer fuel elements at three different locations.

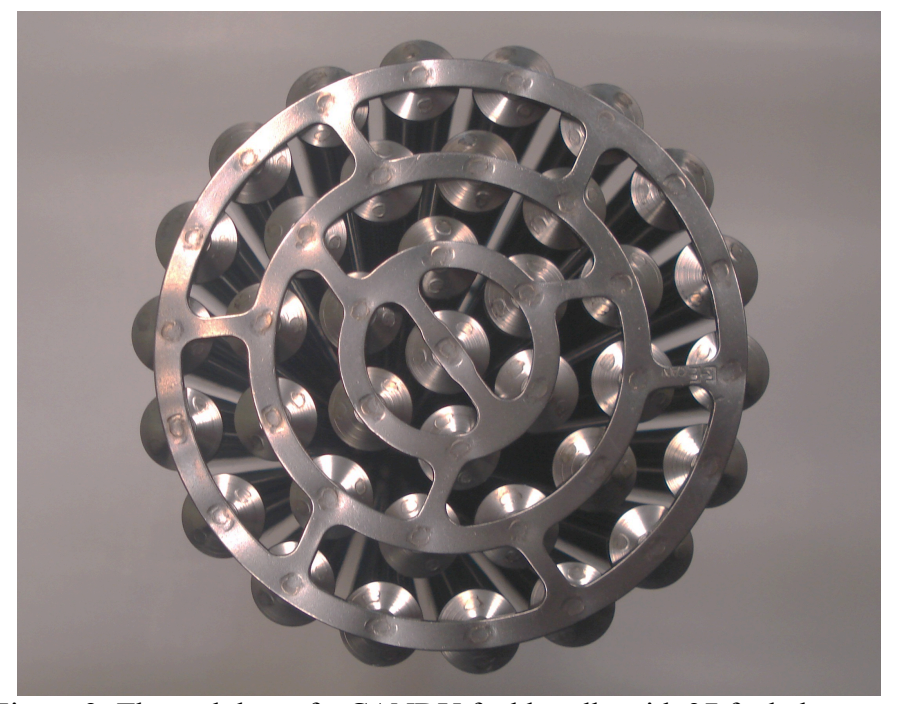


Figure 2: The endplate of a CANDU fuel bundle with 37 fuel elements.

In 1990, one of the fuel bundles in Darlington nuclear power plant was damaged as a result of excessive vibration of the fuel elements. The fuel bundle endplates were found broken and subsequent inspections found severe wear marks in a few fuel channels in Units 1 and 2. Dennier et al. (1994) carried out an extensive test program at Darlington Unit 3 to evaluate the vibration response of the fuel bundles under different flow conditions. They discovered that the cracks were caused by axial response of the fuel bundle which was triggered by the pressure pulsations generated at the primary heat transport (PHT) vane-passing frequency. However, the sever wear marks observed in the fuel channels were caused by the bearing pads of the outer fuel elements as the fuel bundle vibrates due to both turbulence-induced excitation generated by the coolant flow, and pressure pulsations generated by the PHT pump. Moreover, Dennier et al. (1994) showed that the pressure pulsations at the PHT vane-passing frequency were highly reduced when the number of vane impellers changed from five to seven. Therefore, this excitation mechanism is not considered in the current investigation.

Various numerical models have been proposed in order to predict the fuel and fuel channel vibration response to turbulence-induced excitation and the associated fretting wear in the surrounding fuel channel. Païdoussis (1975) developed an elementary mathematical model to predict the dynamic response of a fuel string subjected to axial flow. However, the model was for vertical fuel strings with support conditions different that those expected in CANDU reactors. Yetisir and Fisher (1998) performed a numerical simulation of CANDU fuel bundle to study the effect of turbulence excitation on fretting wear between fuel bundle bearing pads and the surrounding pressure tube using VIBIC (VIbration of Beams with Intermittent Contact), which is a finite element program that was developed by Rogers and Pick (1976) for modelling of heat exchanger tubes with circular clearance supports. Moreover, Yetisir and Fisher (1998) conducted experimental work to validate their simulation results and they suggested that the fuel bundle vibration due to turbulence-induced excitation was not sufficient to produce the same rates of fretting wear damage observed in Darlington nuclear power plant. This confirms the experimental observation of Dennier et al. (1994) that the wear marks observed in the fuel channels at Darlington were caused by both turbulence-induced excitation generated by the coolant flow, and pressure pulsations generated by the PHT pump.

More recently Hassan and Rogers (2005) developed a numerical model to simulate a loosely supported fuel-element subjected to turbulence excitation. They investigated the effects of clearance and preload on the fuel-element response and the predicted work rate. However, Hassan and Rogers (2005) considered only one bearing pad and did not include the effect that neighbouring fuel-elements will have on the fuel bundle vibration response and the predicted wear rate. Therefore, the main objective of this paper is to present a more realistic numerical model to predict the vibration response of a CANDU fuel bundle and the associated fretting wear in the surrounding pressure tube. The model will include the effect that neighbouring fuel-elements will have on the fuel bundle vibration response and the predicted wear rate. The proposed modelling technique can be used in future CANDU reactors to avoid fuel and pressure tube fretting damage due to the aforementioned excitation mechanisms.

1. Tube/Support Interaction Model

The mathematical modelling of the tube/support impact used herein was described in detail and verified by Hassan et al. (2002). Briefly, any support configuration can be modelled by a number of massless bars arranged around the tube, as shown in Figure 3. The i^{th} flat bar is defined by a normal unit vector \hat{e}_{ni} and a radial clearance C_{ri} . The tangential unit vector \hat{e}_{ti} can be obtained by the cross-product of the tube's axial unit vector and \hat{e}_{ni} . Each flat-bar support is attached to a contact-equivalent stiffness element (k_i) and a damper (C_i) . Impact between the tube and the i^{th} support occurs when the tube displacement normal to the flat bar $(w_{ni} = \vec{w} \cdot \hat{e}_{ni})$ exceeds the radial clearance (C_{ri}) . The tube/support overlap is given by:

$$\delta_{ni} = w_{ni} - C_{ri} \tag{1}$$

The normal contact force for the i^{th} flat bar (F_{ci}) can be calculated by:

$$\vec{F}_{ci} = -(k_i \delta_{ni} + sign(\dot{\delta}_{ni})(1.5\alpha |k_i \delta_{ni}|)).\,\hat{e}_{ni}$$
(2)

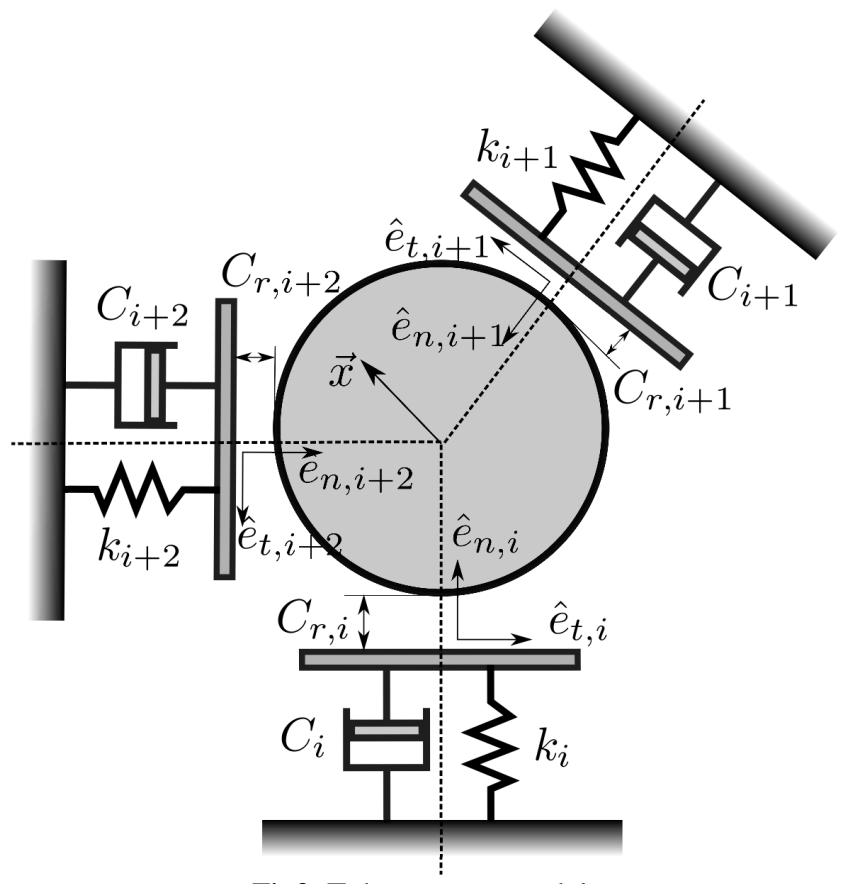


Fig3. Tube-support model.

The first term in the above equation represents the spring force component, which results from considering a concentrated spring at the support point, while the second term accounts for the energy loss during impact. α is an impact damping parameter related to the coefficient of

restitution Saúve and Teper (1987). The current work utilizes the force-balance friction model with the velocity correction technique described in Hassan and Rogers (2005). In this model the sticking friction is checked when the absolute tangential velocity ($|V_t| = |\dot{w}. \hat{e}_{ti}|$) is less than a small limiting velocity (V_o). Friction force during sticking is estimated by:

$$\vec{F}_{fri} = -\left[K(\vec{w}.\,\hat{e}_{ti}) - \vec{F}_{e}.\,\hat{e}_{ti}\right] \tag{3}$$

The term $K(\vec{w}. \hat{e}_{ti})$ in the above equation represents the internal tangential forces at the point of contact. F_e is the external force including turbulence forces which will be further described in Section (2). In or der to confirm the occurrence of sticking, \vec{F}_{fri} must satisfy the inequality $|\vec{F}_{fri}|$ < $\mu_s F_{ci}$ where μ_s is the static friction coefficient. If the aforementioned conditions are not satisfied, the sliding condition prevails and the friction force is calculated by:

$$\vec{F}_{fri} = -\mu_k |\vec{F}_{fri}| \cdot \hat{e}_{ti} \tag{4}$$

where μ_k is the kinetic coefficient of friction.

1.1 Turbulence Excitation

The coolant flow inside the fuel bundles is highly turbulent which induces unsteady forces and causes vibration of fuel bundles inside a channel. In general, fluid excitation due to turbulence is modelled as randomly distributed forces. To implement this approach, the empirically based bounding spectra of turbulence excitation is obtained using the flow velocity, the tube's diameter, and the array geometry. A bounding spectra has been proposed by Smith and Derksen (1998), which utilized in this work to generate the random excitation forces. This power spectral density (PSD) curve is then transformed into a force-time record using an inverse Fourier transform algorithm. The resulting fluctuating forces are Gaussian in nature with a zero mean value. For each flow velocity, two different force versus time records were created representing the fluid excitation in two orthogonal directions. The two force-time records are fully uncorrelated. Turbulence forces were assumed to be fully correlated along the tube span in each direction. The assumption that these forces are fully correlated along the tube length is not entirely accurate. The correlation length of the turbulent forces is typically a few diameters Axisa et al (1990) and Romberg and Popp (1998). Practically, the assumption of a fully correlated turbulent forces is a conservative one.

2. Finite Element Implementation

The tube is discretized into finite beam elements, and the proper boundary conditions are applied. To calculate the time history of the tube response, a pseudo-force algorithm is used. In this procedure, fluidelastic forces are assumed to be known and the corresponding response is computed using the standard finite element solution of the beam equation:

$$[M]\{\ddot{w}\} + [C]\{\dot{w}\} + [K]\{w\} = \{F_t(t)\} + \{F_{imp}(\dot{w}, w, t)\}$$
 (5)

where F_t represents the external turbulence force vector. F_{imp} is the impact force vector that includes all normal contact (F_c) and friction forces (F_{fr}) due to all supports. Eqn. 5 is then

discretized and integrated via the Newmark method. Turbulent forces are used to compute the tube response. Based on the computed response, impact forces are calculated at the support locations.

3. Clearance Measurements

The clearance between the centre bearing pads and the inside surface of a pressure tube can vary depending on the location of the tube. Figure 4 shows the clearance measurements for a bundle performed by Dennier et al. (1995). Each curve represents the centre pad-to-pressure tube clearance for an element at several bundle orientations. The curves show that fuel elements are in contact with pressure tube when they locate in the range of -60° to +60° measured from the bottom location. As expected the maximum clearance occurs at 180° location which represents the diametral differences between the bundle outer and pressure tube inner diameters. In addition, measurements of the clearance between the side and top (tall) spacers were performed. The measurements distribution, shown in Figures 5a and 5b, shows a maximum clearance of 0.37 mm and 0.82 mm for the side and top spacers, respectively.

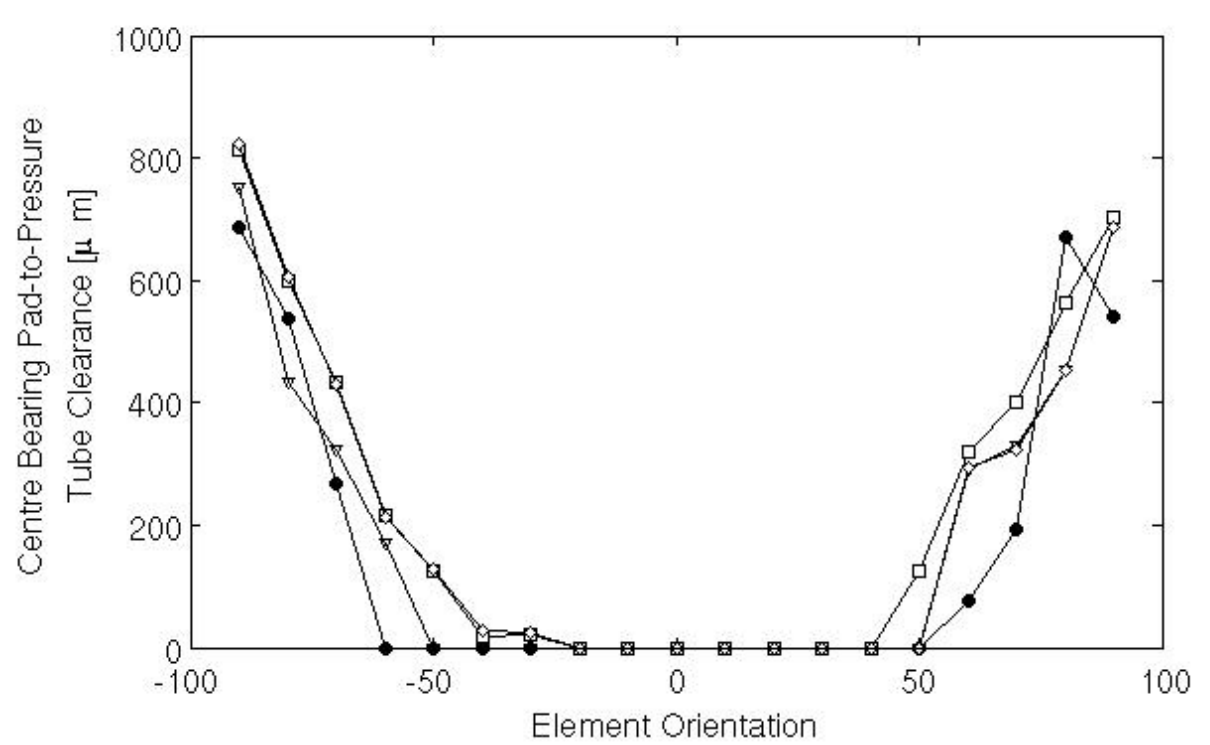


Figure 4: Distribution of the clearances between the centre bearing pads and the pressure tube, from Dennier et al. (1995).

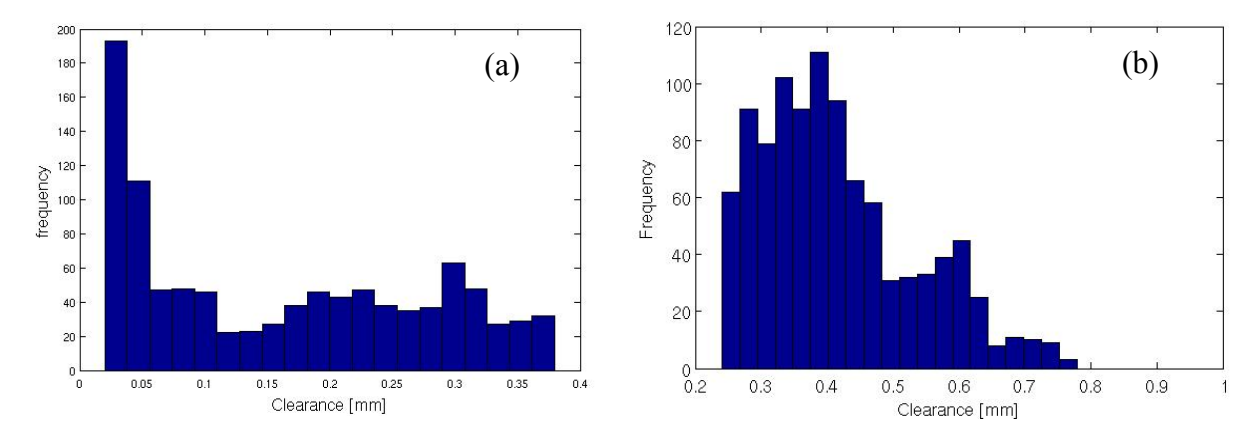


Figure 5: Distributions of the measured clearances between. (a) for the side spacers; and (b) for the top (tall) spacers.

4. Fuel Element Model

The fuel element considered here, as shown in Figure 6, consists of a flexible clamped-clamped beam which is loosely supported at three locations. At location 1 and 3 the loose supports represent the bearing pads of one fuel element of a CANDU fuel bundle resting on the bottom inside surface of a pressure tube. At the mid-span, shown in Figure 7, the loose supports represents a) bearing pad that separates the fuel bundle from the pressure tube, b) 2 side spacers which separate fuel element and the two neighbouring side tubes c) 2 tall spacers which separate fuel element and the two upward neighbouring tubes. The geometric and material properties are shown in Table 1.

Table 1: Properties of the fuel element Geometric properties

Ocometric properties	
Length	L = 495mm
Outside diameter of fuel element	$d_o = 13.1 \text{mm}$
Inside diameter of fuel element	$d_i = 12.2 \text{ mm}$
Inside radius of pressure tube	$r_{p} = 51.5 \text{mm}$
	•
Contact properties	
Contact stiffness	$k_c = 1 \times 106 \text{ N/m}$
Contact damping coefficient	$\gamma = 0.3 \text{ s/m}$
Kinetic friction coefficient	$\mu = 0.5$
Material properties	
Modulus of elasticity at 265 ° C	E = 80.0 GPa
Poisson's ratio at 265 ° C	v = 0.35
Density of tube material	$\rho tube = 6500 \text{ kg/m3}$
Density of internal material	$\rho_i = 10500 \text{ kg/m}3$
Density of surrounding fluid	$\rho_{\rm f} = 775 \text{ kg/m}3$
Modal damping ratio	$\zeta = 3.0\%$
End rotational stiffness	$k_{rot} = 40 \text{ N m/rad}$

The model consisted of 30 three-dimensional beam elements where the axial translation and torsional rotation degrees of freedom were constrained at all nodes. The lateral y (vertical) and z (horizontal) translation degrees of freedom were fixed to zero at the two ends. Rotational springs represent the rotational stiffness of the endplates about the y and z axes.

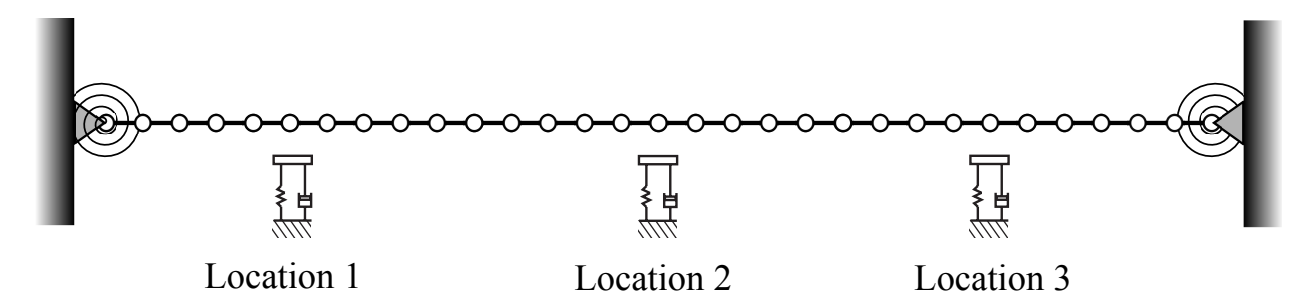


Figure 6: Boundary conditions of the fuel bundle.

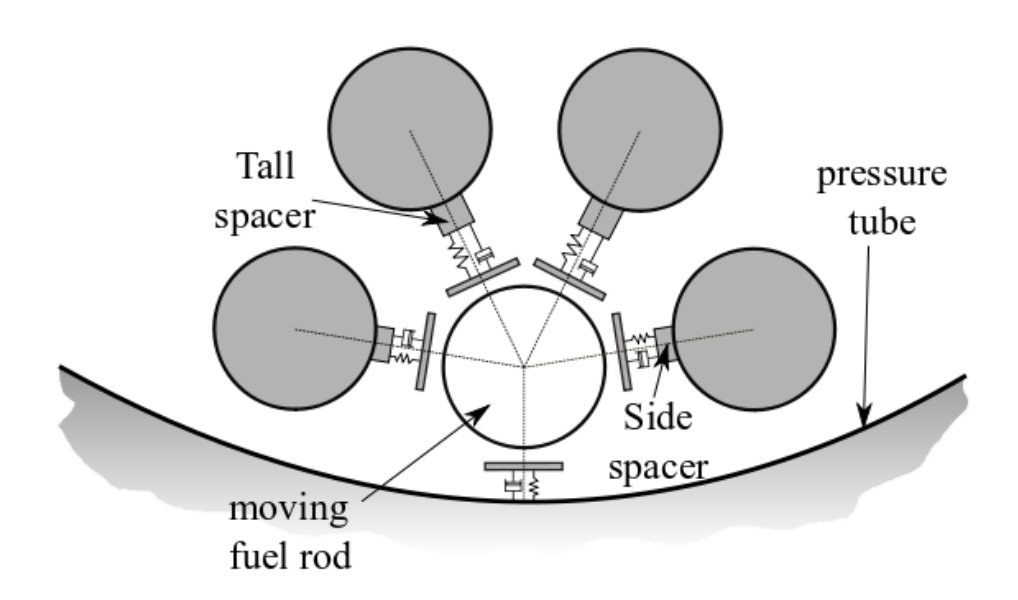


Figure 7: Boundary conditions of one fuel element at the fuel bundle mid-span.

It was demonstrated by several studies (Yetisir and Fisher 1997, Hassan and Rogers 2005) that clearance and preloads are the two principal factors that affect fretting wear. In addition, the interaction between clearances at impact locations greatly affects the resulting wear rate at each location. As shown earlier these clearances vary randomly. In order to account to each possible combination a very large number of deterministic simulations needs to be performed. In addition, an estimate of the predicted distribution of wear in the presence of these clearance variation is of interest.

In order to treat this variability in the impact location conditions more realistically and take into account these uncertainties, which influence the resulting work rate and response predictions, probability density functions (PDF) representing these clearances and preloads are utilized. In previous attempts (Saúve et al 1997 and Rubiolo 2006) normal distributions were assumed to represent the clearance distribution. In the current work, probability distribution functions are proposed for each of impact location (7 locations). These PDFs are constructed using the measured clearances at the spacers and bearing pads. The inversion Method was utilized to generate the random clearance values. It should be noted that for the bearing pad a negative clearance represents a preload which is calculated based on the total weight of the bundle and the orientation of the fuel element. These preloads are estimated from the random variables rather than being imposed to the simulation. 1000 samples were generated randomly and were found to adequately represent the full set of the clearance variations.

6. Results

6.1 Deterministic Simulation

Figure 8 shows the work rate at the center bearing pad as a result of the fuel bundle vibration due to turbulence-induced excitation. It should be noted that this simulation was performed without the side and tall spacers shown in Figure 7. It is clear from Figure 8 that the work rate of the bearing pad increases as the pre-load "negative clearance" decreases and reaches a value of about 32 mW at a clearance value of 0.1 mm. The value of the pre-load was determined from the distribution of the fuel bundle weight on the bearing pads. As the clearance between the bearing pad and the pressure tube increases the work rate decreases.

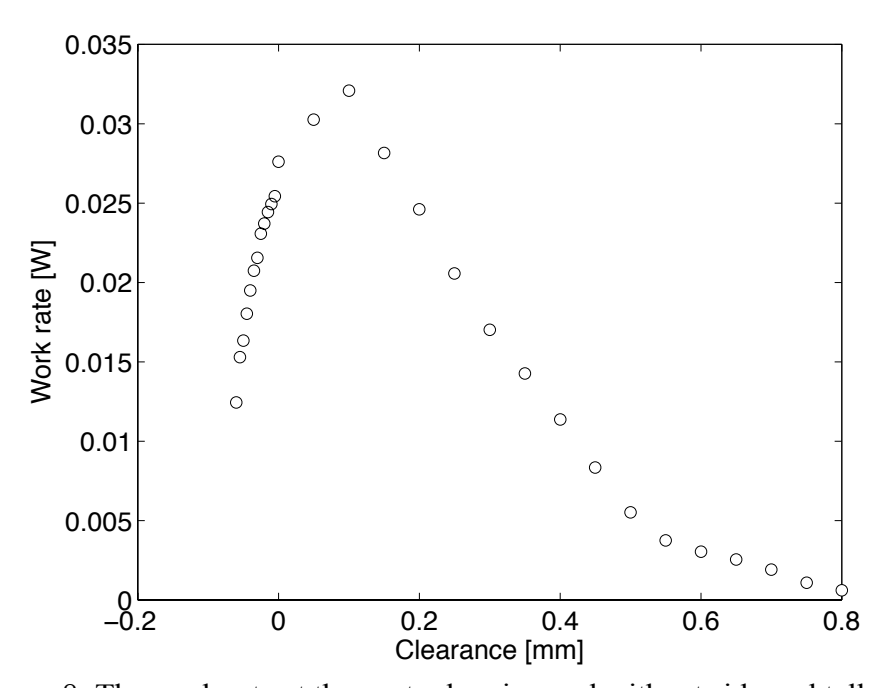


Figure 8: The work rate at the center bearing pad without side and tall spacers.

Figure 9 shows samples of the fuel element midspan response and impact forces at the bearing pad and side spacers at two different bearing pad clearances (0.0 and 0.2 mm). The side spacer clearance was kept at 0.2 mm. For the 0.0 mm clearance case, tube response exhibits single

sided contact characteristics (Figure 9a). High impact forces with frequent contact between the fuel element and the pressure tube are evident as shown in Figure 9c. On the other hand less contact between the fuel element and side tubes as shown in Figure 9e. For the bearing pad clearance case of 0.2 mm, the response exhibits double-side contact characteristics in the horizontal direction with the side tubes, as shown in Figure 9b. Lower impact forces with smaller contact frequency with the pressure cylinder are observed (Figure 9d). However, the impact intensifies at the two side spacers with more frequent contacts (Figure 9f).

Figure 10 shows the effect of adding the side spacers on the work rate at the center bearing pad. The clearance between the side spacers and the fuel element is 0.2 mm. It is clear that adding the side and tall spacers reduced the maximum work rate to almost half its value before adding the side and tall spacers. Moreover, the maximum work rate occurs at a smaller clearance value, about 0.075 mm, between the bearing pad and the pressure tube.

6.2 Probabilistic Simulation

Because of the variation in the measured clearance values, a probabilistic simulation was performed to determine the effect of the clearance between the bearing pads and the pressure tube, and between the side and tall spacers on the work rate at the bearing pads, as shown in Figure 11 and 12, respectively. It is clear from Figure 11 that as the clearance value between the bearing pads and the pressure tube increases the maximum work rate value of the bearing pad decreases. Similar behaviour can be seen in Figure 12, as the clearance between the side and top (tall) spacers increases the work rate at the bearing pad decreases. Moreover, it seems that for this case the work rate has a lower bound that decreases as the clearance increases. The minimum work rate reaches zero at a clearance of about 0.3 mm.

7. Summary

A numerical model is developed to predict the vibration response of a CANDU fuel bundle and the associated fretting wear in the surrounding pressure tube. The clearance between the buttons of the inner fuel elements, and between the bearing pads of the outer fuel elements and the pressure tube is measured for a CANDU fuel bundle with 37 fuel elements. The results shows that as the pre-load decreases the work rate of the bearing pad increases and reaches a value of about 32 mW at a clearance value of 0.1 mm for the case without both the side and top (tall) spacers. When the side and top spacers are added, the maximum work rate of the bearing pad decreases to 0.016 W and it occurs at a smaller clearance value of 0.075 mm.

Some variation among the measured clearance values is observed. Therefore, a probabilistic approach has been utilized to account for the variation of the measured clearances at all contact locations. The probabilistic simulation shows that as the clearance value between the bearing pads and the pressure tube, and between the side spacers increases the maximum work rate value of the bearing pad decreases.

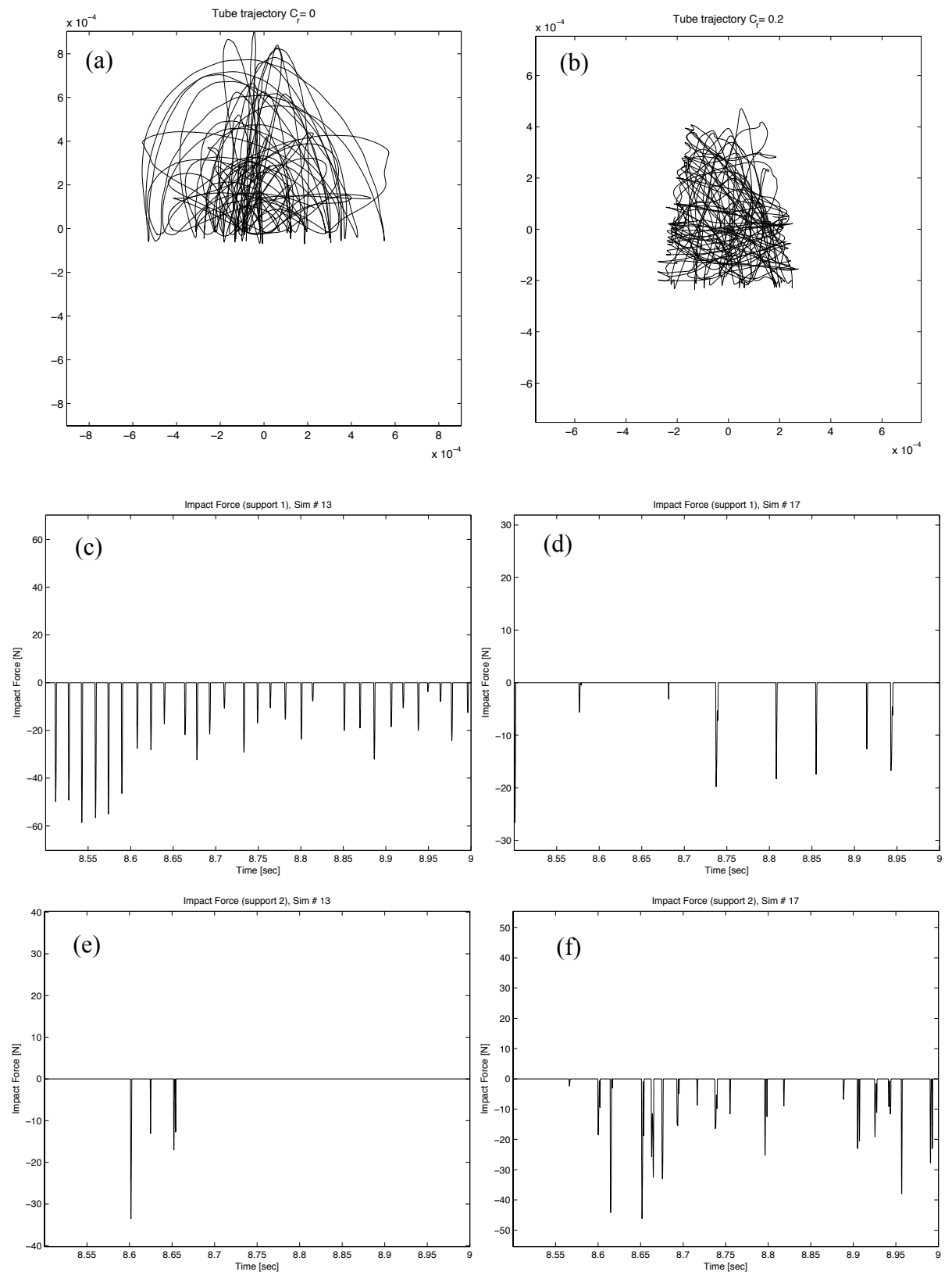


Figure 9: Trajectory and impact forces at the bearing pad and side spacers at 0.0 mm and 0.2 mm clearance between the bearing pad and the pressure tube.

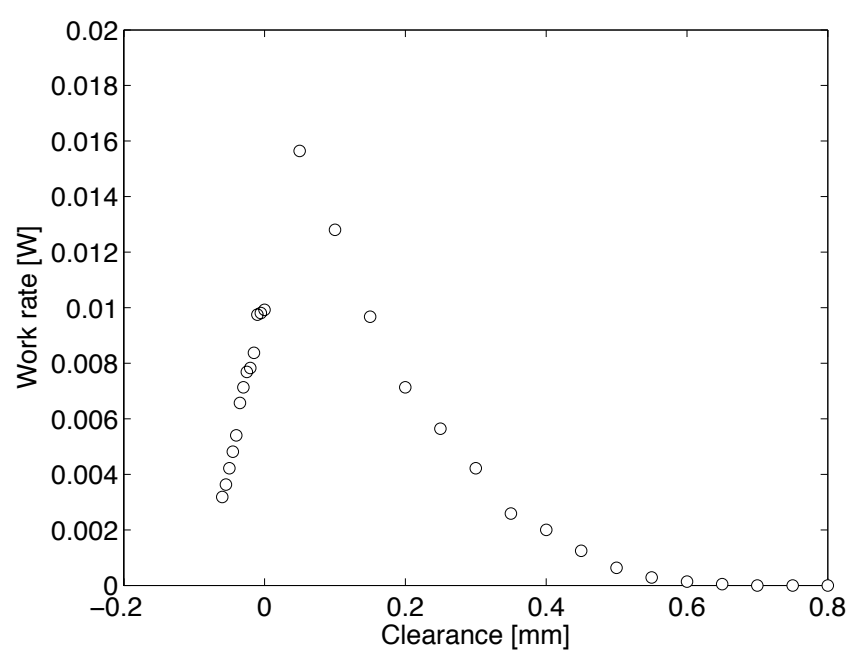


Figure 10: The work rate at the center bearing pad after adding side spacers with a clearance value of 0.2 mm.

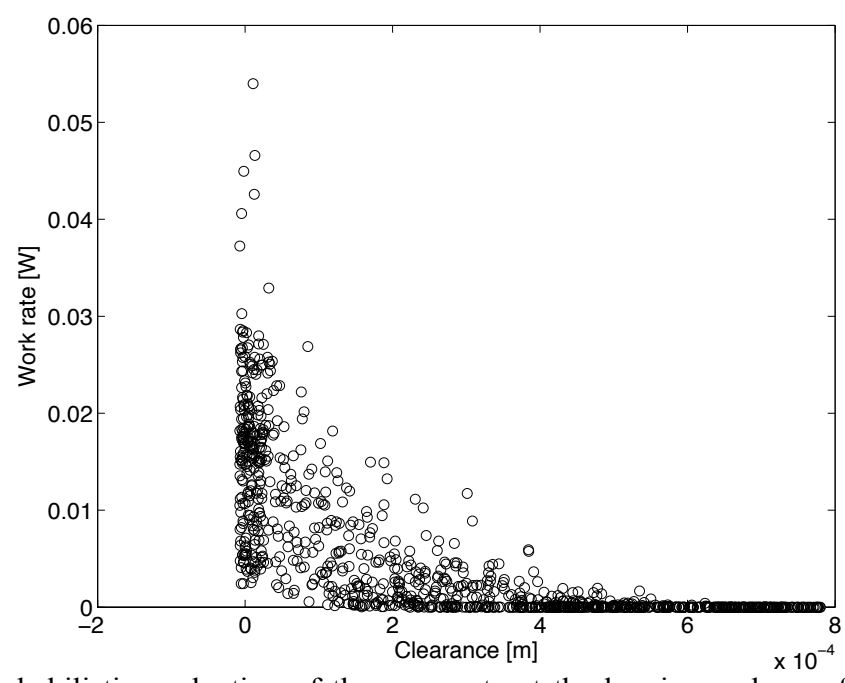


Figure 11: Probabilistic evaluation of the wear rate at the bearing pad as a function of the clearance between the bearing pads and the pressure tube.

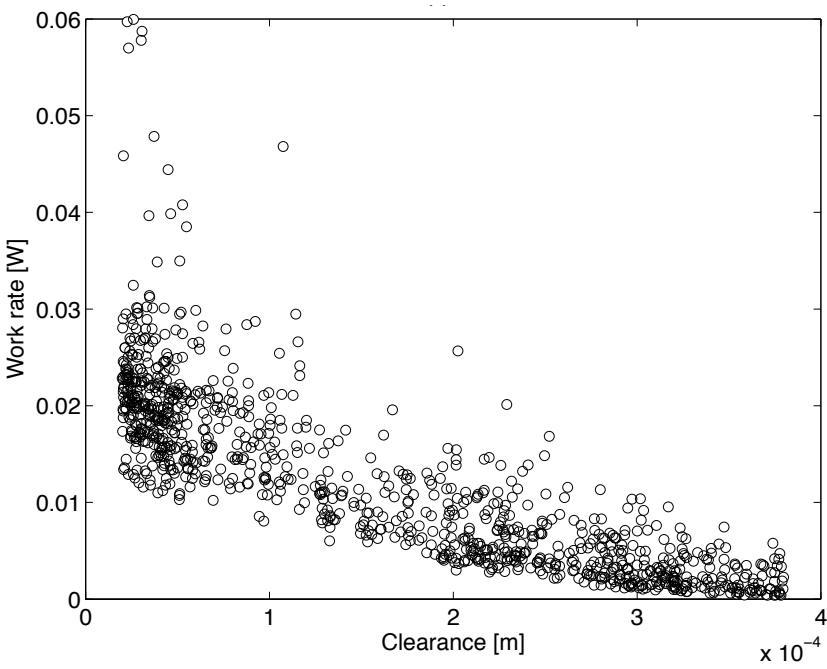


Figure 12: Probabilistic evaluation of the wear rate at the bearing pad as a function of the clearance between the side and tall spacers and the fuel element.

8. Acknowledgement

The authors thankfully acknowledge the financial support provided by the Natural Sciences and Engineering Research Council of Canada (NSERC).

9. References

- [1] D. Dennier, A.M. Manzer, I. Oldaker, E. Kohn, "Deformation and fretting wear of CANDU bundles from DNGS-3 vibration tests", Proceedings of the 15th Annual Conference of the Canadian Nuclear Society, 1994.
- [2] M. Paidoussis, "Mathematical model for the dynamics of an articulated string of fuel bundles in axial flow", International Conference on Structure Mechanics in Reactor Technology, 3rd, Trans, 1975.
- [3] Yetisir, M. and Fisher, N.J., "Prediction of pressure tube fretting-wear damage due to fuel vibration", Nuclear Engineering and Design 176, 261–271, 1997.
- [4] Rogers, R.J. and Pick, R.J. "On the dynamic spatial response of a heat exchanger tube with intermittent baffle contacts" Nuclear Engineering Design, 36 (1), 81–90, 1976.
- [5] Hassan, M. and Rogers, R. Friction Modelling of Preloaded Tube Contact Dynamics Nuclear Engineering and Design, 2005, 235, 2349-2357.
- [6] Hassan, M.; Weaver, D. & Dokainish, M. A Simulation of the Turbulence Response of Heat Exchanger Tubes in Lattice-Bar Supports Journal of Fluids and Structures, 2002, 16, 1145-1176.

- [7] Saúve, R. & Teper, W. Impact Simulation of Process Equipment Tubes and Support Plates a Numerical Algorithm ASME Journal of Pressure Vessel Technology, 1987, 109, 70-79.
- [8] Smith, B., and Derksen, D., "Measurement of Steady and Unsteady Hydrodynamic Loads on Nuclear Fuel Bundle", Journal of Fluids and Structures (1998) 12, 475-489.
- [9] Axisa, F.; Antunes, J. & Villard, B. Random Excitation of Heat Exchanger Tubes by Cross Flows Journal of Fluids and Structures, 1990, 4, 321-341.
- [10] Romberg, O. & Popp, K. Influence of upstream turbulence on the fluidelastic instability of a parallel triangular tube bundle Journal of Fluids and Structures, 1998, 12, 153-169.
- [11] Dennier, D., Manzer, A.M., Kohn, E., "Characteristics of CANDU Fuel Bundles That Caused Pressure Tube Fretting at the Bundle Midplane", 16th Annual CNS Conference, Saskatoon, Saskatchewan, 1995 June 4-7.
- [12] Saúve, R. G., Morandin, G. and Savoia, D. Pettigrew, M. (ed.) Probabilistic Methods for the Prediction of Damage in Process Equipment Tubes under Nonlinear Flow Induced Vibration Flow-Induced Vibration and Noise, ASME, 1997, 53-2, 283-289.
- [13] Rubiolo, P., 2006, Probabilistic prediction of fretting-wear damage of nuclear fuel rods, Nuclear Engineering and Design 236 (2006) 1628-1640.